Prospective life cycle assessment of sodium-ion batteries made from abundant elements

DOI: 10.1111/jiec.13452

RESEARCH ARTICLE

JOURNAL OF INDUSTRIAL ECOLOGY WILEY

Prospective life cycle assessment of sodium-ion batteries made from abundant elements

Sanna Wickerts[1] | Rickard Arvidsson[1] | Anders Nordelöf[1,2] | Magdalena Svanström[1] | Patrik Johansson[3,4]

[1]Environmental Systems Analysis, Chalmers University of Technology, Gothenburg, Sweden

[2]Institute of Transport Economics, Oslo, Norway

[3]Materials Physics, Department of Physics, Chalmers University of Technology, Gothenburg, Sweden

[4]ALISTORE – European Research Institute, Amiens, France

Correspondence
Rickard Arvidsson, Environmental Systems Analysis, Chalmers University of Technology, 412 96 Gothenburg, Sweden.
Email: rickard.arvidsson@chalmers.se

Editor Managing Review: Deepak Rajagopal

Funding information
Energimyndigheten, Grant/Award Number: 50099-1

Abstract

Batteries are enablers for reducing fossil-fuel dependency and climate-change impacts. In this study, a prospective life cycle assessment (LCA) of large-scale production of two different sodium-ion battery (SIB) cells is performed with a cradle-to-gate system boundary. The SIB cells modeled have Prussian white cathodes and hard carbon anodes based only on abundant elements and thus constitute potentially preferable options to current lithium-ion battery (LIB) cells from a mineral resource scarcity point of view. The functional unit was 1 kWh theoretical electricity storage capacity, and the specific energy density of the cells was 160 Wh/kg. Data for the cathode active material come from a large-scale facility under construction and data for the SIB cell production is based on a large-scale LIB cell gigafactory. For other SIB cell materials, prospective inventory data was obtained from a generic eight-step procedure developed, which can be used by other LCA practitioners. The results show that both SIB cells indeed have considerably lower mineral resource scarcity impacts than nickel-manganese-cobalt (NMC)-type LIB cells in a cradle-to-gate perspective, while their global warming impacts are on par. Main recommendations to SIB manufacturers are to source fossil-free electricity for cell production and use hard carbon anodes based on lignin instead of phenolic resin. Additionally, since none of the assessed electrolytes had clearly lower cradle-to-gate impacts than any other, more research into SIB electrolyte materials with low environmental and resource impacts should be prioritized. An improvement of the SIB cell production model would be to obtain large-scale production data specific to SIB cells.

KEYWORDS
industrial ecology, LCA, mineral resource scarcity, Prussian white, upscaling

1 | INTRODUCTION

Batteries are enablers for reducing society's fossil-fuel dependency and climate-change impacts by replacing fossil fuel with battery-electric vehicles powered by fossil-free electricity, such as solar and wind power (Knobloch et al., 2020). Furthermore, a steady supply of such power can be ensured by stationary energy storage in batteries (Larcher & Tarascon, 2015). To fulfill the projected demand for batteries, the total battery production needs to increase by a factor of 14 between 2018 and 2030 (from 180 to 2600 GWh), preferably alongside improvements in environmental sustainability (Edström et al., 2020). The currently dominating rechargeable battery technology is lithium-ion batteries (LIBs), which have sustainability issues related to cell production and raw material extraction. The former is energy intensive, but the impacts from cell production can be greatly reduced given large-scale production based on fossil-free energy (Chordia et al., 2021). The issues of extraction then remain. With the projected increase in demand for LIBs, lithium availability might constitute a future bottleneck for their production (Ambrose & Kendall, 2020). Similar concerns exist for cobalt and nickel, which are important materials in some LIBs (Fu et al., 2020; Xu et al., 2020). Cobalt has also been connected to negative social impacts, such as poor working conditions in small-scale Congolese mining (Sovacool, 2019). Several LIB materials are considered critical in terms of high supply risks and economic importance for the European Union, such as lithium, cobalt, and natural graphite (Blengini et al., 2020). This criticality probably applies to other parts of the world as well.

Because of these sustainability issues, several next-generation battery technologies are under development. One example is sodium-ion batteries (SIBs), which in terms of specific energy density are currently inferior to LIBs, but have other advantages; sodium is about 1000 times more abundant than lithium in Earth's crust (Rudnick & Gao, 2014), and less concentrated to certain regions (Usiskin et al., 2021). SIBs can make use of the LIB development since similar production processes and facilities can be utilized, making the scale-up of SIB production potentially swift (Xie et al., 2020). Yet, the life cycle environmental and resource impacts of SIBs need to be thoroughly evaluated to identify hotspots and trade-offs.

Several previous life cycle assessments (LCAs) of SIBs and their components have been conducted, none of which covers the exact same cells as this study. Peters et al. (2016) assessed an SIB pack with cylindrical cells (128 Wh/kg at cell level), containing a layered oxide cathode ($Na_{1.1}(Ni_{0.3}Mn_{0.5}Mg_{0.05}Ti_{0.05})O_2$), a hard carbon anode, and a sodium hexafluorophosphate ($NaPF_6$)-based organic electrolyte. Several hard carbon precursors were assessed: sugar, starch, cellulose, organic waste, and petroleum coke. Jasper et al. (2022) assessed the life cycle impacts of a battery home storage system powered by the SIB considered by Peters et al. (2016), using data from that study. Peters et al. (2021) evaluated prismatic SIB cells with a hard carbon anode from petroleum coke, an $NaPF_6$-based organic electrolyte, and five different cathode materials with different specific energy densities: $Na_{1.1}(Ni_{0.3}Mn_{0.5}Mg_{0.05}Ti_{0.05})O_2$ with 172 Wh/kg, $Na_{2/3}(Mn_{0.95}Mg_{0.05})O_2$ with 157 Wh/kg, $Na_{1.05}(Ni_{0.33}Mn_{0.33}Co_{0.33})_{0.95}O_2$ with 136 Wh/kg, $Na_2Fe(Fe(CN)_6)$ with 124 Wh/kg, and $Na_4MnV(PO_4)_3$ with 153 Wh/kg. In a Ph.D. thesis by Wellings (2021), an SIB pack with a pouch cell (specific energy at 133 Wh/kg) was assessed, which contained a metal oxide cathode, a graphite anode, and a $NaPF_6$-based organic electrolyte. Carvalho et al. (2022) assessed a coin SIB cell with an $Na_{0.44}MnO_2$ cathode and an MXene ($Ti_1Al_1TiC_{1.85}$) anode. They considered a laboratory-scale production scenario with 0.126 Wh/kg specific energy at cell level, and a hypothetical industrial-scale scenario with 0.429 Wh/kg. Schneider et al. (2019) assessed an SIB cell (ca. 100−150 Wh/kg depending on scenario) with a hard carbon anode, an $NaNi_{1/3}Co_{1/3}Mn_{1/3}O_2$ cathode, and an $NaPF_6$-based organic electrolyte. These studies cover a range of different SIB cells, but none of them relied on data from manufacturers and only one (Peters et al., 2021) performed a detailed assessment of mineral resource scarcity.

Turning to LCA studies of SIB components, Peters et al. (2019) compared several feedstocks for hard carbon intended for SIBs: waste apple pomace, waste tires, and synthetic resin. Similarly, Liu et al. (2021) assessed hard carbons for SIBs, with biomass as feedstock to two production routes: direct pyrolysis, and hydrothermal carbonization followed by pyrolysis. Malara et al. (2021) assessed another SIB anode material, namely electrospun iron oxide-based fibers. Rey et al. (2022) conducted an LCA of a $Na_3V_2(PO_4)_3$ cathode material intended for SIBs, and Mozaffarpour et al. (2022) assessed the SIB cathode material $Na_3MnCO_3PO_4$ produced by ball milling, a hydrothermal method, or a stirring-assisted hydrothermal method. Baumann et al. (2022) conducted a screening LCA of 42 SIB cathode materials, considering climate-change impacts of precursor materials and energy requirements during production. Hofmann et al. (2022) presented LCA results for a range of propylene carbonate-based liquid electrolytes intended for SIBs. Finally, Trotta et al. (2022) assessed a glucose-based hard carbon anode for SIBs. These studies cover many important SIB components, but again none of them relied on data from manufacturers and only two studies (Peters et al., 2019; Rey et al., 2022) performed significant analyses of mineral resource scarcity.

In contrast to previous LCA studies on SIBs and SIB components, this study assesses large-scale production of SIB cells based on manufacturing data representing large-scale cathode active material production and large-scale LIB cell production adapted to SIB cells. In contrast to most previous LCA studies on SIBs and SIB components, this study also has a strong focus on mineral resource scarcity. Two SIB cells developed explicitly to contain elements abundant in the Earth's crust ($\gtrsim$1%), atmosphere, or biosphere are assessed. Both have Prussian white ($Na_2Fe_2(CN)_6$) cathodes, hard carbon anodes, and organic electrolytes with sodium salts. The metallic elements (iron, sodium, and aluminum) are extracted in large amounts annually compared to other battery materials, resulting in low supply risk (Vaalma et al., 2018). One of the cells also contains more bio-based and fluorine-free materials. The rationale for this is to reduce the dependency on fossil resources (Vanholme et al., 2013) and to avoid (eco)toxic effects of fluorinated materials, including fluorinated polymers such as polyvinylidene fluoride (PVdF) (Lohmann et al., 2020), which is commonly used as binder material in battery cells (Zou & Manthiram, 2020). It can thus be hypothesized that these SIB cells have low mineral resource scarcity impacts

in a life cycle perspective. However, is this true and do the SIB cells also have comparatively low environmental impacts? To partially answer these questions, the aims of this study are to (i) conduct a cradle-to-gate LCA to identify hotspots for further improvements of the SIB cells based on manufacturer data for cell and cathode active material production, and (ii) benchmark against cradle-to-gate impacts of other SIB and LIB cells.

2 | METHODS

SIBs constitute an emerging technology, that is, a radically novel, fast-growing technology with potentially prominent impacts, surrounded by considerable uncertainty (Rotolo et al., 2015). According to the scales for technology and manufacturing readiness levels (TRLs and MRLs, respectively) in van der Hulst et al. (2020), SIBs are currently at approximately TRL/MRL = 7–8, corresponding to pilot-scale production. In this study, the two SIB cells were assessed in a prospective LCA where they were modeled at a future point in time when they have reached technological maturity and large-scale production (TRL = 9 and MRL = 10), as described by Arvidsson et al. (2018). Considering the recent interest in SIBs, reaching such levels during 2025—2030 does not seem unlikely.

A cradle-to-gate system boundary was considered, covering raw material extraction and battery production up until the cells leave the manufacturing facility (Figure 1). This system boundary was chosen since large uncertainties exist regarding the future use and end of life of SIBs. Manufacturers of SIB cells and components are an important intended audience of this study, in addition to battery researchers and LCA practitioners assessing batteries as such or in various applications. The foreground system therefore consisted of the production of the cathode active material, cathode, anode, electrolyte, cell assembly, and cell formation, all for which data was obtained from manufacturers, either directly through this study or through a previous LCA by Chordia et al. (2021). A global geographical system boundary was considered, meaning that global averages were generally applied for material and energy production. A functional unit of 1 kWh of theoretical storage capacity was chosen, which quantifies the main function of a rechargeable battery, namely to store energy (Porzio & Scown, 2021), and is common in cradle-to-gate LCAs of batteries; see, for example, Dai et al. (2019) and Chordia et al. (2021). Considering the aims of the study, an attributional or process-based perspective to the inventory modeling was adopted, meaning that environmentally relevant linear physical flows to and from the product system are quantified (Finnveden et al., 2009; Yang, 2019). Calculations were performed in the software OpenLCA (GreenDelta, version 1.10.3).

Two approaches to allocate impacts between co-products were applied: physical (mass-based) allocation and an approach where all impacts are allocated to the main product (i.e., the product assessed and its precursors), sometimes called the main-product-bears-all-burden approach (Hermansson et al., 2020). Mass allocation is a common approach and can be seen as a base scenario, while the main-product-bears-all-burden approach is less common and constitutes a worst-case scenario for the studied product (Guinée et al., 2021). The latter also represents a possible future where constituents and precursors of the SIB cells are considered the absolutely most important co-products of their production processes, thus carrying the vast majority of the impacts. Following Sander-Titgemeyer et al. (2023), economic allocation was not applied due to the challenges of estimating future prices. Substitution is another option for handling multifunctionality, but was not applied in this study since it has been associated with consequential LCA by several scholars, for example, Schaubroeck et al. (2021) and Ekvall (2019), whereas this is an attributional LCA.

Although the end-of-life stage was not included in this cradle-to-gate study, the cutoff approach was applied for recycled materials in upstream production processes, meaning that recycled materials are only responsible for impacts during recycling processes (Ekvall & Tillman, 1997).

Section 2.1 describes the two cells assessed. Sections 2.2 and 2.3 describe the prospective foreground and background system modeling, respectively. Section 2.4 describes the life cycle impact assessment (LCIA) methods applied.

2.1 | Sodium-ion battery cells assessed

Information about the two SIB cells considered was obtained from a collaboration with an SIB cell manufacturer (Table 1). The two cells are here named "Cell 1" and "Cell 2," the latter being the cell with a higher share of bio-based and fluorine-free materials. Both are pouch cells with a capacity of 5 Ah and a theoretical specific energy density of 160 Wh/kg.

The anode active material is hard carbon, which is among the best-performing materials for SIB anodes (Xie et al., 2020). Phenolic resin is the raw material in Cell 1 and lignin from softwood is the raw material in the more bio-based Cell 2. Phenolic resin is of fossil origin, while lignin is bio-based and the second most abundant polymer in the biosphere (Dessbesell et al., 2020). Prussian white, which is a manufactured material that contains only geochemically abundant elements, is the cathode active material in both cells and is recognized as promising for SIBs (Tapia-Ruiz et al., 2021). A binder is present in both the anode and cathode: PVdF in Cell 1, and a mixture of carboxy-methyl cellulose (CMC) and styrene-butadiene rubber (SBR) in Cell 2. Cellulose is the most abundant polymer in the biosphere (Dessbesell et al., 2020), whereas the SBR is mainly made from fossil materials.

In Cell 1, the electrolyte is $NaPF_6$ in ethylene carbonate and diethyl carbonate solvents, which is a common electrolyte option for SIBs (Ponrouch et al., 2015). However, if coming into contact with water, $NaPF_6$ can degrade to form corrosive and toxic hydrogen fluoride, leading to electrolyte degradation and safety concerns (Barnes et al., 2020). As an alternative, sodium bis(oxalato)borate (NaBOB) in triethyl phosphate is the electrolyte

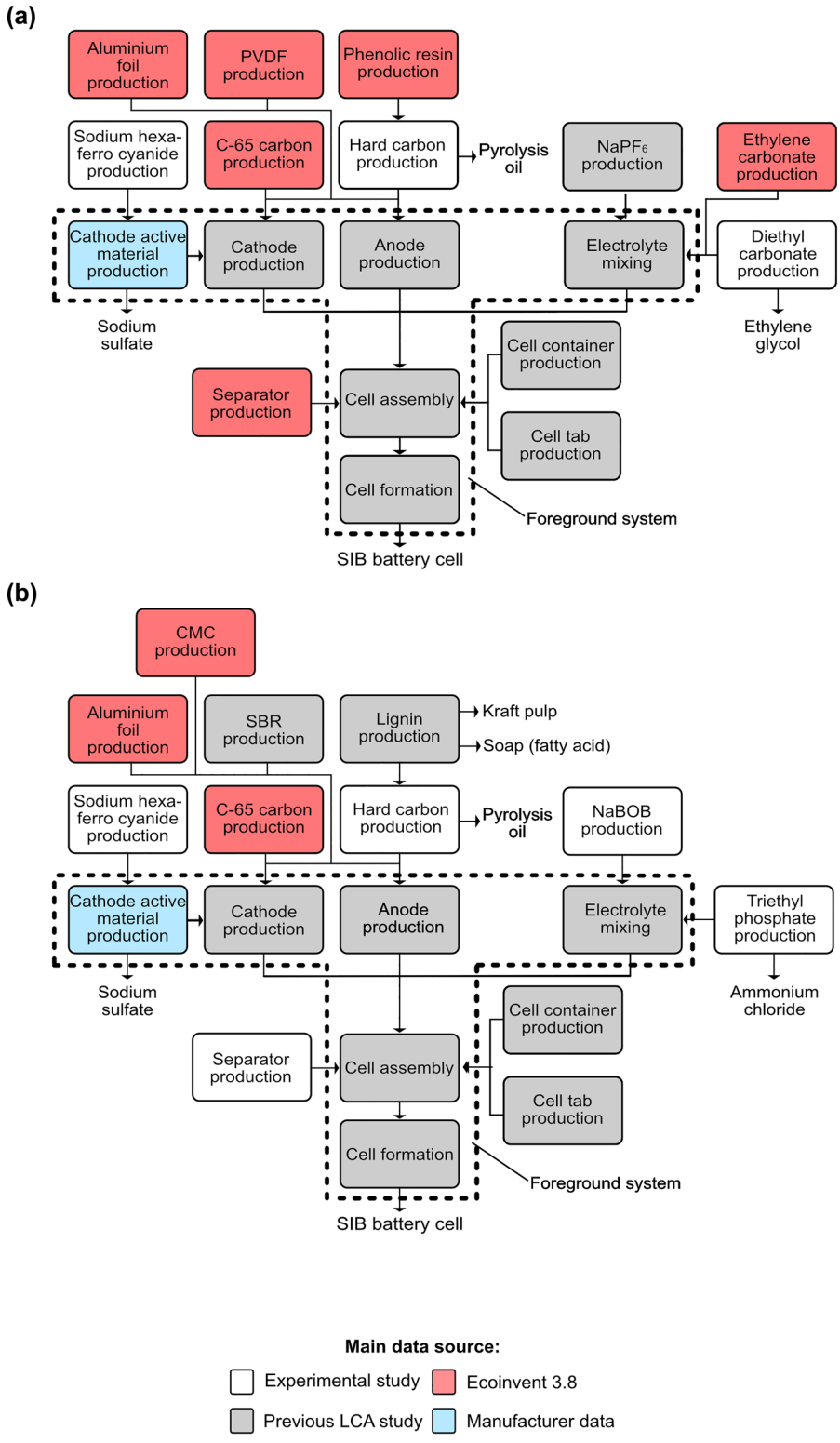

FIGURE 1 Flowchart and main data sources for the sodium-ion battery cells studied: (a) Cell 1 and (b) Cell 2. C-65, carbon black powder; CMC, carboxy-methyl cellulose; NaBOB, sodium bis(oxalato)borate; $NaPF_6$, sodium hexafluorophosphate; PVdF, polyvinylidene fluoride; SBR, styrene-butadiene rubber.

TABLE 1 Compositions of the two sodium-ion battery cells.

Cell materials (wt%)	Cell 1	Cell 2
Anode active material (20%)	Hard carbon made from phenolic resin	Hard carbon made from lignin
Cathode active material (33%)	Prussian white	
Conductive additive C65 (1%)	Carbon	
Binder (2%)	PVdF	CMC and SBR
Electrolyte (27%)	$NaPF_6$ (1 M) in ethylene carbonate and diethyl carbonate (1:1)	NaBOB (0.4 M) in triethyl phosphate
Separator (4%)	Polyolefin based	Cellulose based
Current collectors (7%)	Aluminum foil	
Pouch and tabs (6%)	Aluminum and plastic	

Abbreviations: C65, carbon black powder; CMC, carboxy-methyl cellulose; NaBOB, sodium bis(oxalato)borate; $NaPF_6$, sodium hexafluorophosphate; PVdF, polyvinylidene fluoride; SBR, styrene-butadiene rubber.

in Cell 2. NaBOB shows promising results regarding toxicity and flammability (Tapia-Ruiz et al., 2021), but contains the geochemically rare boron. Polyolefin-based separators are commonly used in battery cells (Luo et al., 2021), including Cell 1. In Cell 2, the separator is instead made from abundant cellulose, which has been shown to have promising properties (Luo et al., 2021).

2.2 | Prospective LCI modeling of the foreground system

The foreground system consists of the cell and cathode active material production, which were modeled based on large-scale production facilities currently under construction. The cell production was assumed to take place in a large-scale gigafactory like that modeled in Chordia et al. (2021), with a capacity of 16 GWh/year. While this model was originally developed for an NMC811 LIB cell, it is considered relevant since SIB production requires similar equipment and LIB facilities will be able to switch to producing SIBs (Tapia-Ruiz et al., 2021; Usiskin et al., 2021). The model was adapted for the SIB cells, for example, by changing to SIB-specific inputs. In cell production, the anode, cathode, and electrolyte are produced and assembled into a cell by stacking the anodes and cathodes on top of each other with a separator in between. Subsequently, the stacked components are sealed in a pouch, which is injected with electrolyte. The cells then undergo formation, meaning that they are charged and discharged several times to create a protective layer between the anode and the electrolyte.

For the cathode active material Prussian white, data was obtained from a manufacturer. The production takes place by decomposing sodium ferrocyanide using sulfuric acid, followed by sodium enrichment by sodium sulfite (Brant et al., 2018). Hydrogen cyanide is also produced in the process, which is reacted with sodium hydroxide and iron sulfate to produce more sodium ferrocyanide precursor that is cycled back to the main reactor. The co-product sodium sulfate is also produced, which is accounted for in the mass-based allocation.

The electricity supply to the cell assembly and the cathode active material production will vary in the future and will also depend on the available supply where these processes take place. Most electricity mixes will likely see reduced carbon intensities in the future due to the ongoing transition of the energy system to mitigate climate impacts (IEA, 2022). In addition to this, sourcing of "green" electricity through tariffs is an option already today. For these reasons, two what-if scenarios (Börjesson et al., 2006) were considered for electricity supply to the foreground system. This first is a moderate scenario based on a mixture of energy sources with a medium-emission intensity (from a 2023 perspective), modeled with the current average electricity mix in the EU as proxy (ca. 400 g CO_2 eq/kWh). The second is an optimistic scenario based on renewable, flow-type energy sources with low-emission intensity, modeled with pure wind power as proxy (ca. 20 g CO_2 eq/kWh).

Details about the modeling of the foreground system can be found in Supporting information S1, including unit-process data for the anode production, cathode production, Prussian white production, electrolyte production, cell assembly, and cell formation.

2.3 | LCI modeling of the background system

Several products in the background system have mature production processes, for example, sodium hydroxide. For these, production was assumed to remain the same when SIB cells are produced at large scale considering the relatively near-future time horizon of the study (2025–2030). They were therefore modeled as described in the Ecoinvent database (version 3.8) or in previous LCA studies. Since the aluminum current collectors are similar to those of LIB cathodes, their production was modeled as in a previous LCA of LIB cells (Chordia et al., 2021), where the aluminum input was modeled as primary metal only due to high material quality requirements. Data for the SBR production was also obtained from Chordia et al.

(2021). Pouch and aluminum tabs are also similar to those of current LIB cells, thus their production data was obtained from a previous LCA of LIBs (Ellingsen et al., 2014), with the aluminum modeled as primary for these two components as well. For $NaPF_6$, data was obtained from a previous LCA of an SIB cell (Peters et al., 2016), which in turn is a modified Ecoinvent dataset for the production of the corresponding lithium salt ($LiPF_6$). Data for the CMC binder and the polyolefin-based separator was obtained from Ecoinvent, and the PVdF binder was approximated using the Ecoinvent process for the similar fluoropolymer polyvinylfluoride.

For modeling the production of materials with immature production processes in the background system, an eight-step procedure based on Piccinno et al. (2016) and Arvidsson et al. (2019) was developed. Piccinno et al. (2016) provided a framework for upscaling process steps, but no detailed guidance on stepwise implementation in unit-process modeling. Arvidsson et al. (2019) provided a stepwise procedure for unit-process modeling of emerging chemicals, but no detailed guidance on calculations in each step. These two approaches are combined. In step (i), a plausible synthesis for the material is identified from experimental articles and patents. In step (ii), a process flowchart is drawn based on the synthesis description. In step (iii), the equipment likely to be applied in scaled-up variants of the processes in the flowchart is identified. In step (iv), reactant inputs are calculated based on data provided in the synthesis descriptions—in cases of insufficient data, stoichiometric calculations are performed, and the result is modified using yields. If no specific yield is identified, a default yield of 95% is applied, following Wernet et al. (2012). In step (v), inputs of solvents and other auxiliary inputs are estimated. Since a reduction in solvent use can be expected after upscaling, −20% as recommended by Piccinno et al. (2016) was applied. As the remaining solvent can be recirculated in upscaled processes, a recirculation rate of 68% provided by Capello et al. (2005) was applied for organic solvents. In step (vi), co-product amounts are obtained from the synthesis descriptions or stoichiometric calculations, and waste amounts are calculated by mass balances. In step (vii), emissions are calculated. Process emissions are rarely reported in synthesis descriptions and are difficult to estimate since they are process and reaction specific (Piccinno et al., 2016). In this study, only emissions of gaseous substances formed in reactions were considered and assumed to be released to air. In step (viii), energy requirements of the process steps and equipment identified in steps (ii) and (iii) are calculated using equations provided by Piccinno et al. (2016). The steps are summarized in Figure 2.

This stepwise procedure was applied to input materials not yet produced at large scale. The synthesis of hard carbon was modeled based on a process simulation of biomass pyrolysis by Liu (2022). For this pyrolysis process, different hard carbon yields have been reported, which was considered in a sensitivity analysis. Data for the production of the phenolic resin precursor is available in Ecoinvent, while data for the lignin precursor was obtained from a previous LCA by Culbertson et al. (2016). The production of NaBOB was modeled based on Shiyou et al. (2019) and Zavalij et al. (2003), involving reactions between boric acid, oxalic acid, and sodium hydroxide, as well as purification with acetonitrile. The diethyl carbonate production was modeled based on Huiquan et al. (2015) and Wang et al. (2014); ethylene oxide, ethanol, and carbon dioxide react over a potassium iodide catalyst. The triethyl phosphate production was modeled based on Xiaoming et al. (2013), in which phosphorus trichloride is reacted with ethanol, ammonia, and oxygen. The cellulose-based separator production was modeled based on Du et al. (2019), in which cellulose is cross-linked with epichlorohydrin in an alkaline solvent. The sodium hexaferrocyanide production was modeled based on information from the cathode active material manufacturer and Wiedeman et al. (1972), involving reaction between hydrogen cyanide, sodium hydroxide, and iron sulfate.

Detailed modeling of all materials with immature production processes in the background system can be found in Supporting Information S1.

2.4 | Life cycle impact assessment

The following impact categories from ReCiPe 2016 were assessed with a hierarchist value perspective: global warming, fossil resource scarcity, mineral resource scarcity, terrestrial acidification, freshwater eutrophication, ozone formation, fine particulate matter formation, stratospheric ozone depletion, and water consumption (Huijbregts et al., 2016). The three first-mentioned impact categories were considered particularly relevant, and their results are therefore presented in the main article, while the others are presented in Supporting Information S1. Global warming is an urgent environmental issue (IPCC, 2021) and is often recommended for inclusion in LCA of batteries (Zackrisson, 2021). Fossil resource scarcity was selected to investigate whether the more bio-based Cell 2 requires less fossil resources than Cell 1 from a cradle-to-gate perspective, since there might be upstream fossil resource use not visible from the cell compositions. Mineral resource scarcity is also frequently recommended for inclusion in LCA of batteries (Zackrisson, 2021) and was selected to investigate whether the high content of geochemically and otherwise abundant materials in the studied SIB cells gives low mineral resource scarcity in a cradle-to-gate perspective. The surplus ore potential (SOP) indicator is used to assess mineral resource scarcity in ReCiPe 2016 (Huijbregts et al., 2016), and considers the additional ore required to obtain the same amount of resource in the future (Vieira et al., 2017). Note that the SOP indicator does not provide characterization factors for every elementary flow related to the cells, such as the sodium in the Prussian white and the fossil raw materials used to produce Cell 1′s hard carbon anode. The hierarchist value perspective is selected since it is an often-employed middle-ground scenario reflecting a level of evidence considered acceptable by international bodies. However, for all indicators from ReCiPe 2016, the sensitivity to the other two value perspectives (individualist and egalitarian) was also assessed.

In addition, since mineral resource scarcity can be assessed from several perspectives (Sonderegger et al., 2020), we included a complementary indicator with an explicit long-term perspective, which is considered particularly relevant in a prospective study: the crustal scarcity indicator (CSI), which considers the concentration of elements in Earth's crust as a proxy for their future scarcity (Arvidsson, Söderman et al., 2020).

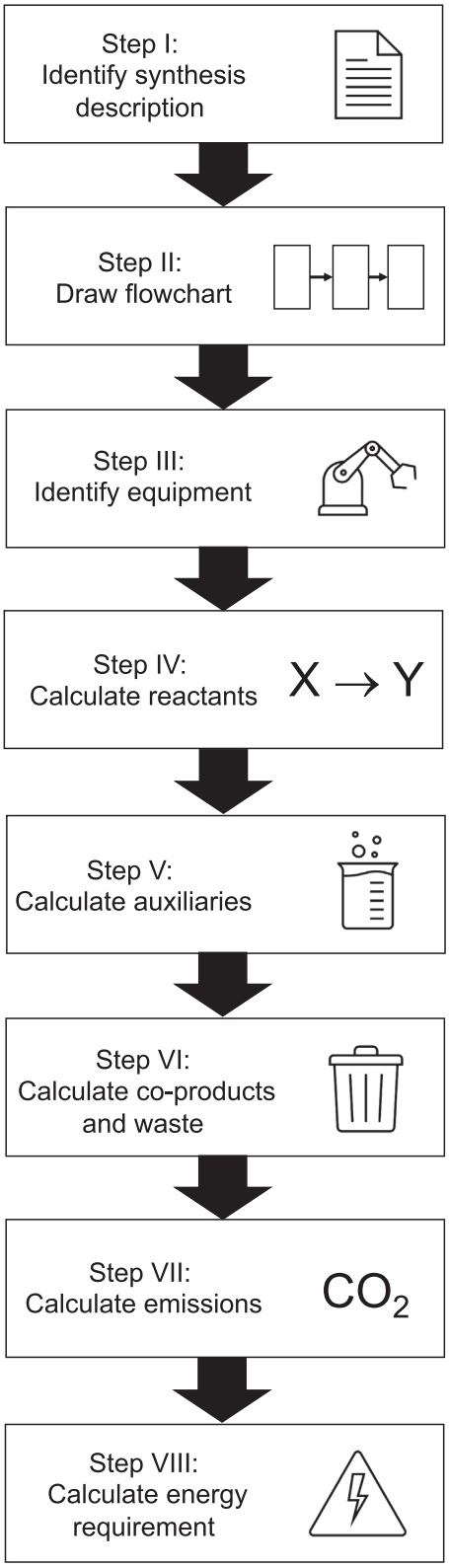

FIGURE 2 Eight-step procedure for deriving prospective unit-process inventory data for materials with immature production processes in the background system.

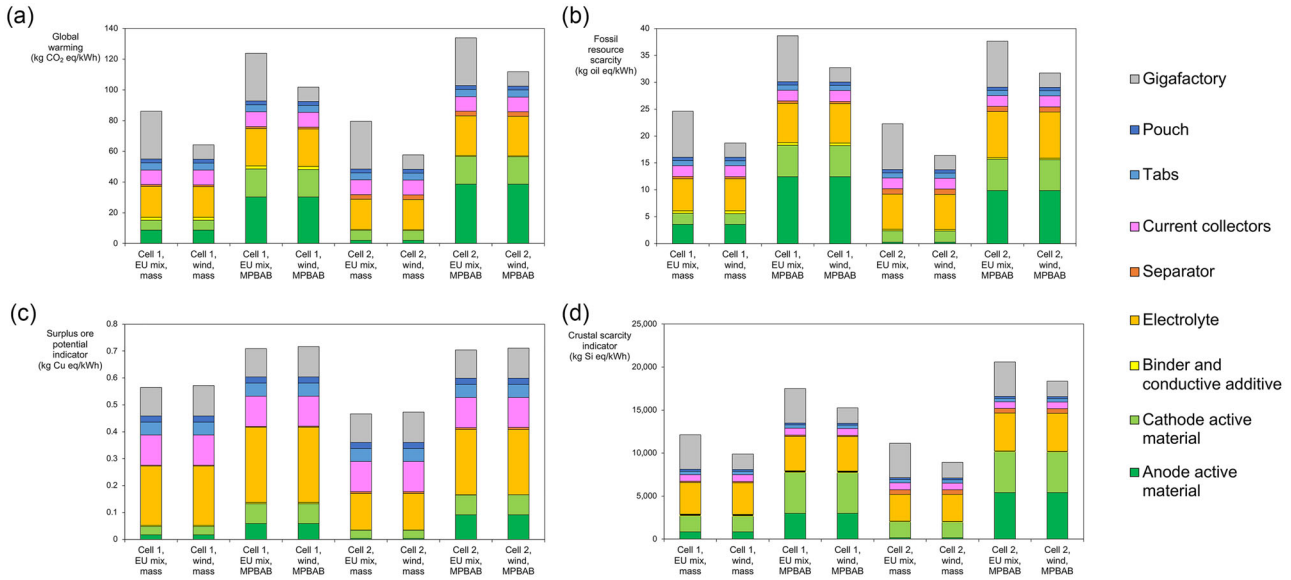

FIGURE 3 Cradle-to-gate results for Cells 1 and 2 regarding (a) global warming, (b) fossil energy scarcity, (c) the surplus ore potential indicator, and (d) the crustal scarcity indicator. Scenarios consider variations in electricity mix in the foreground system (EU mix or wind power) and allocation method (mass, mass allocation or MPBAB, main product bears all burden). The data used to create the figure is provided in Supporting Information S1.

3 | RESULTS AND DISCUSSION

Figure 3 shows cradle-to-gate results for Cells 1 and 2 with different electricity supplies to the foreground system (EU mix or wind power) and different allocation approaches (mass allocation or main product bears all burden). There is no single dominant hotspot, but several parts of the product system contribute notably to most impact categories: anode active material production (hard carbon), cathode active material production (Prussian white), the gigafactory, electrolyte production, and current collector production. Other parts of the product system contribute negligibly to most impact categories: binder and conductive additive production, tabs production, separator production, and pouch production. This applies also to most impact categories not shown in Figure 3, see Supporting Information S1. Consequently, the difference in binder and separator composition matters little for the difference in cradle-to-gate impacts between Cell 1 and Cell 2. A more detailed comparison of impacts from the two separators can be found in Supporting Information S1.

In Section 3.1, cradle-to-gate results for global warming and fossil energy scarcity are discussed in more detail, with a focus on the main contributors noted above. In Section 3.2, cradle-to-gate results for the SOP and the CSI are similarly discussed. Numerical results for all included impact categories and sensitivity analysis results are presented in Supporting Information S1, along with result graphs showing elementary flow contributions.

3.1 | Global warming and fossil resource scarcity

The gigafactory is an important contributor to global warming and fossil resource scarcity (Figure 3a,b), mainly through high electricity use. Therefore, changing to a fossil-free electricity supply, such as wind power, notably reduces global warming and fossil resource scarcity. This applies to all scenarios and is in line with previous research on large-scale production of LIBs (Chordia et al., 2021). The global warming and fossil resource scarcity results are similar for Cell 1 and Cell 2, despite the differences in composition. With mass-based allocation, the lignin-based hard carbon anode in Cell 2 has lower global warming and fossil resource scarcity compared to the phenolic resin-based hard carbon anode in Cell 1. This could become even lower by avoiding fossil inputs upstream. The only direct fossil input to the pulp mill in the dataset used for lignin production was natural gas heat to the lime kiln (Culbertson et al., 2016), which might be replaced by a fossil-free heat source. The contributions from the electrolytes in Cell 1 and Cell 2, however, are approximately equal. Thus, the ambition to avoid the fluorine-containing $NaPF_6$ does not seem to lead to notable reductions in global warming and fossil energy scarcity in a cradle-to-gate perspective. The contribution from diethyl carbonate comes mainly from the production, distillation, and waste treatment of the ethanol input, which might be possible to optimize further. The contribution from NaBOB comes mainly from the production and distillation of acetonitrile as well as the production of oxalic acid. Optimizing the input of acetonitrile solvent might thus reduce this contribution. For triethyl phosphate, the contribution comes mainly from the primary reactants: phosphorus

chloride, ethanol, and ammonia. $NaPF_6$ and ethylene carbonate have only minor contributions. A more detailed comparison of impacts from the two electrolytes can be found in Supporting Information S1.

The differences in results between mass allocation and the main-product-bears-all-burden approach show that two materials are sensitive to allocation: hard carbon and Prussian white. For hard carbon, there is an allocation point in the pyrolysis between hard carbon and pyrolysis oil, with a mass ratio of 1:2.5 (Liu, 2022). In addition, for the lignin-based hard carbon, there is a prior allocation point in the kraft pulp mill between lignin, kraft pulp, and soap consisting of fatty acids, with a mass ratio of approximately 4:35:1 (Culbertson et al., 2016). This means that with mass-based allocation, most of the impacts from hard carbon production are allocated to the pyrolysis oil and kraft pulp. In the main-product-bears-all-burden scenarios, hard carbon is the main product and bears all burden of the pyrolysis and pulp mill, so the contribution of the lignin-based hard carbon becomes notably higher. In these scenarios, the lignin-based and phenolic resin-based hard carbons have contributions of similar magnitude, with the impacts of the lignin-based hard carbon coming mainly from sodium chlorate, wood chips, and natural gas used in the pulp mill. A more detailed comparison of impacts between the two hard carbons can be found in Supporting Information S1.

In the Prussian white production, the two co-products are Prussian white and sodium sulfate. With mass allocation, these products receive approximately equal shares of upstream impacts. With the main-product-bears-all-burden approach, the contribution of Prussian white increases notably. In 2023, sodium sulfate could be bought online at prices around 0.1€/kg, while the future price of Prussian white is expected to be notably higher. Economic allocation would thus probably give results similar to those of the main-product-bears-all-burden approach. The impacts of Prussian white come mainly from the hydrogen cyanide and sodium hydroxide inputs, regardless of the allocation approach.

3.2 | Mineral resource scarcity

For the SOP indicator (Figure 3c), a shift from the EU mix to wind power in the foreground system has negligible influence since this indicator does not include the carbonaceous raw materials required for, for example, coal power. Cells 1 and 2 get similar SOP results, but the two allocation approaches give notably different results. The hard carbon and Prussian white both get higher SOP with the main-product-bears-all-burden approach, as discussed in Section 3.1. In addition, the SOP of the electrolyte components diethyl carbonate and triethyl phosphate increase notably with the main-product-bears-all-burden approach as they otherwise share burdens with their co-products ethylene glycol and ammonium chloride, respectively. The SOP of Prussian white comes mainly from metals (copper, nickel, and molybdenum) deriving from sulfuric acid, sodium hydroxide, and iron sulfate production. For triethyl phosphate, phosphorus extracted for the phosphorus trichloride production contributes the most. For diethyl carbonate, iodine in the potassium iodide catalyst contributes the most. The SOP of the aluminum current collectors is—unsurprisingly—dominated by aluminum. The electrolyte salt $NaPF_6$ also contributes notably to the SOP of Cell 1, mainly due to the phosphorus used for producing the phosphorus pentachloride precursor.

The main contributors to the SOP of the SIB cells are aluminum for the current collectors and tabs, as well as gallium, which is extracted from the same ore as the aluminum as a co-product, and its resource impact is fully allocated to the aluminum in the Ecoinvent dataset for aluminum production. In addition, the iodine for the potassium iodide catalyst in diethyl carbonate production contributes notably for Cell 1, and phosphorus for the triethyl phosphate production contributes notably for Cell 2. All these elements except gallium have relatively low SOP characterization factors (Huijbregts et al., 2016), but the comparatively large amounts used make them important contributors.

The CSI follows a similar pattern as the global warming and fossil resource scarcity (Figure 3d)—wind power and mass allocation reduce impacts, while Cells 1 and 2 get similar results since the two electrolytes have roughly similar impacts. The main contributors to the CSI are the energy use of the gigafactory, the Prussian white production, hard carbon (for the main-product-bears-all-burden approach), $NaPF_6$ (for Cell 1), NaBOB (for Cell 2), and triethyl phosphate (for Cell 2). For the gigafactory energy use, the largest contributor is coal for coal power with the EU mix, which disappears in the wind power scenarios. For Prussian white, sodium chloride extracted for sodium hydroxide is the main contributor. For $NaPF_6$, the largest contributor is fluorspar, that is, the source of fluorine. For NaBOB, the main contributor is the boron-containing mineral colemanite, but fossil inputs to the acetonitrile production also contribute notably. For triethyl phosphate, phosphorus extracted to produce the phosphorus trichloride contributes the most.

The main contributing elementary flows to the CSI of the SIB cells are coal, oil, tellurium, sodium chloride, and the boron-containing colemanite (for Cell 2). All these minerals except tellurium and colemanite have relatively low characterization factors in the CSI method (Arvidsson, Chordia et al., 2020), but they are extracted in large amounts to supply the SIB product system and therefore receive high impact.

3.3 | Comparison to other battery cells

Results for the two SIB cells are here compared to cradle-to-gate results from other LCA studies of SIBs and LIBs. The LCA study on SIB cells by Peters et al. (2016) applied a previous version of the ReCiPe method, but the global warming indicator is similar across the versions. They also applied the hierarchist value perspective and mass-based allocation, resulting in 140 kg CO_2 eq/kWh, close to the highest cradle-to-gate results

TABLE 2 Comparison to selected cradle-to-gate life cycle assessment studies of sodium-ion and lithium-ion battery cells.

Study	Cathode, anode, electrolyte salt	Specific energy (Wh/kg)	Electricity mix	Global warming (kg CO_2 eq/kWh)	Mineral resource scarcity (kg Cu or Si eq/kWh)
Sodium-ion battery cells					
Cell 1, this study	Prussian white Hard carbon $NaPF_6$	160	EU/wind	64–120	SOP: 0.57–0.72 CSI: 9900–18,000
Cell 2, this study	Prussian white Hard carbon NaBOB	160	EU/wind	58–130	SOP: 0.47–0.71 CSI: 8900–21,000
Peters et al. (2016)	Layered oxide Hard carbon $NaPF_6$	128	EU	140	n.a.
Peters et al. (2021)	Several Hard carbon $NaPF_6$	124–172	EU	50–90	n.a.
Carvalho et al. (2022)	$Na_{0.44}MnO_2$ MXene $NaPF_6$	0.13–0.43	Italy	5200–56,000	n.a.
Schneider et al. (2019)	$NaNi_{1/3}Mn_{1/3}Co_{1/3}O_2$ Hard carbon $NaPF_6$	ca. 100–150	South Korea	ca. 80–140	n.a.
Lithium-ion battery cells					
Chordia et al. (2021)	NMC811 Graphite $LiPF_6$	210–240	Sweden/South Korea	50–110	SOP: 10 CSI: 65,000
Sun et al. (2020)	NMC622 Graphite $LiPF_6$	180	China	94–120	n.a.
Dai et al. (2019)	NMC111 Graphite $LiPF_6$	197	United States	73	n.a.

obtained with the main-product-bears-all-burden approach in this study (Figure 3a). The comparatively high global warming impact reported in Peters et al.'s study is likely due to a lower specific energy density (128 Wh/kg), a higher impact of the layered oxide cathode compared to the Prussian white, the higher impact of the sugar-based hard carbon, and the EU electricity mix. In the more recent study, Peters et al. (2021) obtained global warming results in the range 50–90 kg CO_2 eq/kWh for cells with different cathode materials and specific energy densities, similar to the range for the mass-allocation scenarios in this study. They included a case similar to Cell 1 in this study with Prussian white, hard carbon, and $NaPF_6$, for which they received 87 kg CO_2 eq/kWh, close to the result at 86 kg CO_2 eq/kWh for Cell 1 with the EU mix and mass allocation in this study. Carvalho et al. (2022) assessed SIB coin cells with much lower cell densities (0.1–0.4 Wh/kg) and thus received much higher impacts: ca. 56,000 kg CO_2 eq/kWh for their lab-scale scenario and ca. 5200 kg CO_2 eq/kWh for their industrial-scale scenario. Results from Schneider et al. (2019) for their SIB cells with an $NaNi_{1/3}Co_{1/3}Mn_{1/3}O_2$ cathode at different performance scenarios are ca. 80–150 kg CO_2 eq/kWh, on the higher side of results from this study. A contributing factor might be the South Korean electricity mix with a high share of fossil-based electricity.

For large-scale production of LIB cells, Chordia et al. (2021) reported the global warming of an NMC811 cell at approximately 110 kg CO_2 eq/kWh for South Korean electricity and 50 kg CO_2 eq/kWh for the Swedish electricity mix, similar to the range in Figure 3a. They also reported an SOP at approximately 10 kg Cu eq/kWh and a CSI at approximately 65,000 kg Si eq/kWh given the Swedish electricity mix. This is more than a factor of 10 higher compared to the SIB cells studied here for the SOP, and at least three times higher for the CSI. Sun et al. (2020) reported the global warming impact of an NMC622 LIB cell at ca. 124 kg CO_2 eq/kWh, or 94 kg CO_2 eq/kWh if recycling benefits were included. They also reported a fossil resource scarcity at 24–28 kg oil eq/kWh, depending on whether recycling was included. This is also similar to the results of this study, albeit at the higher end for global warming. Dai et al. (2019) reported the global warming of an NMC111 LIB cell at ca. 73 kg CO_2 eq/kWh, which is within the range obtained for SIB cells in this study, especially for the mass-based allocation results.

A summary of this comparison can be seen in Table 2. Note that allocation approaches are often not clearly reported in these studies, while this might contribute to differences in results.

4 | CONCLUSIONS

A main conclusion from this study is that the SIB cells based on abundant elements perform better than LIB cells regarding mineral scarcity for the cradle-to-gate system boundary. This is in line with Peters et al. (2021), who also showed that an SIB cell with a Prussian white cathode had lower mineral resource scarcity impacts than LIB cells. They applied the abiotic resource depletion potential (ADP) indicator, which is constructed similarly to the CSI but additionally considers the extraction rate of resources (van Oers et al., 2020). The comparative advantage of SIB cells with Prussian white regarding mineral resource scarcity in a cradle-to-gate perspective is thus confirmed for two additional indicators in this study (the SOP and CSI).

Another main conclusion is that SIB cells with Prussian white cathodes and LIB cells perform similarly for global warming and fossil resource scarcity given a cradle-to-gate system boundary. This is contrary to Peters et al. (2021), who showed that an SIB cell with Prussian white had almost twice the global warming compared to LIB cells: ca. 90 versus ca. 50 kg CO_2 eq/kWh. However, this represents global warming results for LIB cells at the lower end of those reported for large-scale production (Table 2). The comparison in this study suggests that these values represent lower- and upper-end results for LIB and SIB cells, respectively. When the full range is considered, Prussian white-based SIB cells and LIB cells tend to be in the same range.

The two most important recommendations for improvements of the SIB cells are (i) that the gigafactory is powered by a fossil-free electricity supply, and (ii) that the hard carbon anode is produced from lignin instead of phenolic resin. Given a shift to renewable electricity for the gigafactory and a lignin-based anode, the electrolyte would be next up for having a large share of the impacts. Since none of the electrolytes considered in this study was clearly preferable over the other, further research into environmentally benign SIB electrolytes should be prioritized.

The provided cradle-to-gate data and results from this study can be used in future cradle-to-grave studies of SIBs in specific applications. Considerations for doing so are provided in Supporting Information S1. A methodological contribution from this study is the eight-step procedure for obtaining prospective LCI data for background system processes, where approaches from Piccinno et al. (2016) and Arvidsson et al. (2019) were combined. This procedure could be applied by other LCA practitioners for obtaining background system data for materials with immature production processes.

An important step for improving the LCA model in this study would be to obtain large-scale SIB cell manufacturing data. In this study, large-scale manufacturing of LIB cells was adapted to SIB cells on a unit-process level, thus relying on a gigafactory originally designed for LIB cells. For example, SIB cells might require less dry-room facilities during production, which is known to be an energy-intensive part of the LIB cell production (Dunn et al., 2015).

ACKNOWLEDGMENTS

The authors thank the Swedish Energy Agency for financial support (grant No. 50099-1). The authors thank the research center Batteries Sweden (BASE) for providing a platform for collaboration.

CONFLICT OF INTEREST STATEMENT

The authors declare no conflict of interest.

DATA AVAILABILITY STATEMENT

The data that supports the findings of this study are available in the supporting information of this article.

ORCID

Rickard Arvidsson https://orcid.org/0000-0002-9258-0641
Anders Nordelöf https://orcid.org/0000-0002-7455-7341

REFERENCES

Ambrose, H., & Kendall, A. (2020). Understanding the future of lithium. Part 1, resource model. *Journal of Industrial Ecology*, *4*, 80–89. https://doi.org/10.1111/jiec.12949

Arvidsson, R., Chordia, M., Wickerts, S., & Nordelöf, A. (2020). *Implementation of the crustal scarcity indicator into life cycle assessment software (Report No. 2020:05)*. Chalmers University of Technology. https://research.chalmers.se/publication/519861

Arvidsson, R., Kushnir, D., Janssen, M., & Sandén, B. A. (2019). *Prospective inventory modeling of emerging chemicals: The case of photonic materials*. SETAC Europe 29th Annual Meeting, Helsinki, Finland. https://research.chalmers.se/publication/510514

Arvidsson, R., Söderman, M. L., Sandén, B. A., Nordelöf, A., André, H., & Tillman, A.-M. (2020). A crustal scarcity indicator for long-term global elemental resource assessment in LCA. *The International Journal of Life Cycle Assessment*, *25*, 1805–1817. https://doi.org/10.1007/s11367-020-01781-1

Arvidsson, R., Tillman, A.-M., Sandén, B. A., Janssen, M., Nordelöf, A., Kushnir, D., & Molander, S. (2018). Environmental assessment of emerging technologies: Recommendations for prospective LCA. *Journal of Industrial Ecology*, *22*(6), 1286–1294. https://doi.org/10.1111/jiec.12690

Barnes, P., Smith, K., Parrish, R., Jones, C., Skinner, P., Storch, E., White, Q., Deng, C., Karsann, D., Lau, M. L., Dumais, J. J., Dufek, E. J., & Xiong, H. (2020). A non-aqueous sodium hexafluorophosphate-based electrolyte degradation study: Formation and mitigation of hydrofluoric acid. *Journal of Power Sources*, *447*, 227363. https://doi.org/10.1016/j.jpowsour.2019.227363

Baumann, M., Häringer, M., Schmidt, M., Schneider, L., Peters, J. F., Bauer, W., Binder, J. R., & Weil, M. (2022). Prospective sustainability screening of sodium-ion battery cathode materials. *Advanced Energy Materials*, *12*(46), 2202636. https://doi.org/10.1002/aenm.202202636

Blengini, G., El Latunussa, C., & Eynard, U. (2020). *Study on the EU's list of critical raw materials—Final report*. European Commission, Directorate-General for Internal Market, Industry, Entrepreneurship and SMEs. https://data.europa.eu/doi/10.2873/11619

Börjesson, L., Höjer, M., Dreborg, K.-H., Ekvall, T., & Finnveden, G. (2006). Scenario types and techniques: Towards a user's guide. *Futures*, *38*(7), 723–739. https://doi.org/10.1016/j.futures.2005.12.002

Brant, W., Mogensen, R., Younesi, R., & Dechar, F. (2018). *Method for producing a sodium iron(II)-hexacyanoferrate(II) material* (Patent No WO/2018/056890). https://patentscope.wipo.int/search/en/detail.jsf?docId=WO2018056890

Capello, C., Hellweg, S., Badertscher, B., & Hungerbühler, K. (2005). Life-cycle inventory of waste solvent distillation: Statistical analysis of empirical data. *Environmental Science & Technology*, *39*(15), 5885–5892. https://doi.org/10.1021/es048114o

Carvalho, M. L., Mela, G., Temporelli, A., Brivio, E., & Girardi, P. (2022). Sodium-ion batteries with Ti1Al1TiC1.85 MXene as negative electrode: Life cycle assessment and life critical resource use analysis. *Sustainability*, *14*(10), 5976. https://doi.org/10.3390/su14105976

Chordia, M., Nordelöf, A., & Ellingsen, L. A.-W. (2021). Environmental life cycle implications of upscaling lithium-ion battery production. *The International Journal of Life Cycle Assessment*, *26*, 2024–2039. https://doi.org/10.1007/s11367-021-01976-0

Culbertson, C., Treasure, T., Venditti, R., Jameel, H., & Gonzalez, R. (2016). Life cycle assessment of lignin extraction in a softwood kraft pulp mill. *Nordic Pulp & Paper Research Journal*, *31*(1), 30–40. https://doi.org/10.3183/npprj-2016-31-01-p030-040

Dai, Q., Kelly, J. C., Gaines, L., & Wang, M. (2019). Life cycle analysis of lithium-ion batteries for automotive applications. *Batteries*, *4*(48), 1–15. https://doi.org/10.3390/batteries5020048

Dessbesell, L., Paleologou, M., Leitch, M., Pulkki, R., & Xu, C. (2020). Global lignin supply overview and kraft lignin potential as an alternative for petroleum-based polymers. *Renewable and Sustainable Energy Reviews*, *123*, 109768. https://doi.org/10.1016/j.rser.2020.109768

Du, Z., Su, Y., Qu, Y., Zhao, L., Jia, X., Mo, Y., Yu, F., Du, J., & Chen, Y. (2019). A mechanically robust, biodegradable and high performance cellulose gel membrane as gel polymer electrolyte of lithium-ion battery. *Electrochimica Acta*, *299*, 19–26. https://doi.org/10.1016/j.electacta.2018.12.173

Dunn, J. B., Gaines, L., Kelly, J. C., James, C., & Gallagher, K. G. (2015). The significance of Li-ion batteries in electric vehicle life-cycle energy and emissions and recycling's role in its reduction. *Energy & Environmental Science*, *8*(1), 158–168. https://doi.org/10.1039/C4EE03029J

Edström, K., Dominko, R., Fichtner, M., Perraud, S., Punckt, C., Asinari, P., Castelli, I. E., Christensen, R., Clark, S., Grimaud, A., Hermansson, K., Heuer, A., Lorrmann, H., Løvvik, O. M., Vegge, T., Wenzel, W., Bayle-Guillemaud, P., Behm, J., Berg, E., … Weil, M. (2020). *Battery 2030+ roadmap. Inventing the sustainable batteries of the future. Research needs and future actions*. https://battery2030.eu/research/roadmap/

Ekvall, T. (2019). Attributional and consequential life cycle assessment. In B.-C. M. José, F.-B. J. Luis, H. Levente, M. Florin-Constantin, & I. Corneliu (Eds.), *Sustainability assessment at the 21st century* (Chapter 4). IntechOpen. https://doi.org/10.5772/intechopen.89202

Ekvall, T., & Tillman, A.-M. (1997). Open-loop recycling: Criteria for allocation procedures. *The International Journal of Life Cycle Assessment*, *2*(3), 155–162. https://doi.org/10.1007/bf02978810

Ellingsen, L. A.-W., Majeau-Bettez, G., Singh, B., Srivastava, A. K., Valøen, L. O., & Strømman, A. H. (2014). Life cycle assessment of a lithium-ion battery vehicle pack. *Journal of Industrial Ecology*, *18*(1), 113–124. https://doi.org/10.1111/jiec.12072

Finnveden, G., Hauschild, M. Z., Ekvall, T., Guinée, J., Heijungs, R., Hellweg, S., Koehler, A., Pennington, D., & Suh, S. (2009). Recent developments in life cycle assessment. *Journal of Environmental Management*, *91*(1), 1–21. https://doi.org/10.1016/j.jenvman.2009.06.018

Fu, X., Beatty, D. N., Gaustad, G. G., Ceder, G., Roth, R., Kirchain, R. E., Bustamante, M., Babbitt, C., & Olivetti, E. A. (2020). Perspectives on cobalt supply through 2030 in the face of changing demand. *Environmental Science & Technology*, *54*(5), 2985–2993. https://doi.org/10.1021/acs.est.9b04975

Guinée, J., Heijungs, R., & Frischknecht, R. (2021). Multifunctionality in life cycle inventory analysis: Approaches and solutions. In A. Ciroth & R. Arvidsson (Eds.), *Life cycle inventory analysis : Methods and data* (pp. 73–95). Springer International Publishing. https://doi.org/10.1007/978-3-030-62270-1_4

Hermansson, F., Janssen, M., & Svanström, M. (2020). Allocation in life cycle assessment of lignin. *The International Journal of Life Cycle Assessment*, *25*(8), 1620–1632. https://doi.org/10.1007/s11367-020-01770-4

Hofmann, A., Wang, Z., Bautista, S. P., Weil, M., Müller, F., Löwe, R., Schneider, L., Mohsin, I. U., & Hanemann, T. (2022). Comprehensive characterization of propylene carbonate based liquid electrolyte mixtures for sodium-ion cells. *Electrochimica Acta*, *403*, 139670. https://doi.org/10.1016/j.electacta.2021.139670

Huijbregts, M. A. J., Steinmann, Z. J. N., Elshout, P. M. F., Stam, G., Verones, F., Vieira, M. D. M., Hollander, A., Zijp, M., & van Zelm, R. (2016). *ReCiPe 2016 - A harmonized life cycle impact assessment method at midpoint and endpoint level. Report I: Characterization*. Dutch National Institute for Public Health and the Environment (RIVM). https://www.rivm.nl/bibliotheek/rapporten/2016-0104.html

Huiquan, L., Liguo, W., Shumin, X., Fengjiao, L., Peng, H., & Yan, C. (2015). *Method for synthesizing diethyl carbonate and coproducing diol by using carbon dioxide* (Patent No CN104418701A). https://patents.google.com/patent/CN104418701A/en

IEA. (2022). *World energy outlook 2022*. International Energy Agency. https://www.iea.org/reports/world-energy-outlook-2022

IPCC. (2021). Summary for policymakers. In V. Masson-Delmotte, P. Zhai, A. Pirani, S. L. Connors, C. Péan, S. Berger, N. Caud, Y. Chen, L. Goldfarb, M. I. Gomis, M. Huang, K. Leitzell, E. Lonnoy, J. B. R. Matthews, T. K. Maycock, T. Waterfield, O. Yelekçi, R. Yu, & B. Zhou (Eds.), *Climate change 2021: The physical science basis. Contributions of Working Group I to the Sixth Assessment report of the Intergovernmental Panel on Climate Change*. Cambridge University Press. https://www.ipcc.ch/report/sixth-assessment-report-working-group-i/

Jasper, F. B., Späthe, J., Baumann, M., Peters, J. F., Ruhland, J., & Weil, M. (2022). Life cycle assessment (LCA) of a battery home storage system based on primary data. *Journal of Cleaner Production*, *366*, 132899. https://doi.org/10.1016/j.jclepro.2022.132899

Knobloch, F., Hanssen, S. V., Lam, A., Pollitt, H., Salas, P., Chewpreecha, U., Huijbregts, M. A. J., & Mercure, J.-F. (2020). Net emission reductions from electric cars and heat pumps in 59 world regions over time. *Nature Sustainability*, *3*(6), 437–447. https://doi.org/10.1038/s41893-020-0488-7

Larcher, D., & Tarascon, J. M. (2015). Towards greener and more sustainable batteries for electrical energy storage. *Nature Chemistry*, *7*(1), 19–29. https://doi.org/10.1038/nchem.2085

Liu, Y. (2022). *Techno-economic analysis of biomass conversion to hard carbon materials*. KTH Royal Institute of Technology. https://urn.kb.se/resolve?urn=urn:nbn:se:kth:diva-315050

Liu, H., Xu, Z., Guo, Z., Feng, J., Li, H., Qiu, T., & Titirici, M. (2021). A life cycle assessment of hard carbon anodes for sodium-ion batteries. *Philosophical Transactions of the Royal Society A: Mathematical, Physical and Engineering Sciences*, *379*(2209), 20200340. https://doi.org/10.1098/rsta.2020.0340

Lohmann, R., Cousins, I. T., DeWitt, J. C., Glüge, J., Goldenman, G., Herzke, D., Lindstrom, A. B., Miller, M. F., Ng, C. A., Patton, S., Scheringer, M., Trier, X., & Wang, Z. (2020). Are fluoropolymers really of low concern for human and environmental health and separate from other PFAS? *Environmental Science & Technology*, *54*(20), 12820–12828. https://doi.org/10.1021/acs.est.0c03244

Luo, W., Cheng, S., Wu, M., Zhang, X., Yang, D., & Rui, X. (2021). A review of advanced separators for rechargeable batteries. *Journal of Power Sources*, *509*, 230372. https://doi.org/10.1016/j.jpowsour.2021.230372

Malara, A., Pantò, F., Santangelo, S., Antonucci, P. L., Fiore, M., Longoni, G., Ruffo, R., & Frontera, P. (2021). Comparative life cycle assessment of Fe2O3-based fibers as anode materials for sodium-ion batteries. *Environment, Development and Sustainability*, *23*(5), 6786–6799. https://doi.org/10.1007/s10668-020-00891-y

Mozaffarpour, F., Hassanzadeh, N., & Vahidi, E. (2022). Comparative life cycle assessment of synthesis routes for cathode materials in sodium-ion batteries. *Clean Technologies and Environmental Policy*, *24*(10), 3319–3330. https://doi.org/10.1007/s10098-022-02381-3

Peters, J. F., Abdelbaky, M., Baumann, M., & Weil, M. (2019). A review of hard carbon anode materials for sodium-ion batteries and their environmental assessment. *Matériaux & Techniques*, *107*(5), 503. https://doi.org/10.1051/mattech/2019029

Peters, J. F., Baumann, M., Binder, J. R., & Weil, M. (2021). On the environmental competitiveness of sodium-ion batteries under a full life cycle perspective—A cell-chemistry specific modelling approach. *Sustainable Energy & Fuels*, *5*(24), 6414–6429. https://doi.org/10.1039/D1SE01292D

Peters, J. F., Buchholz, D., Passerini, S., & Weil, M. (2016). Life cycle assessment of sodium-ion batteries. *Energy & Environmental Science*, *9*, 1744–1751. https://doi.org/10.1039/c6ee00640j

Piccinno, F., Hischier, R., Seeger, S., & Som, C. (2016). From laboratory to industrial scale: A scale-up framework for chemical processes in life cycle assessment studies. *Journal of Cleaner Production*, *135*(Supplement C), 1085–1097. https://doi.org/10.1016/j.jclepro.2016.06.164

Ponrouch, A., Monti, D., Boschin, A., Steen, B., Johansson, P., & Palacin, M. R. (2015). Non-aqueous electrolytes for sodium-ion batteries. *Journal of Materials Chemistry A*, *3*(1), 22–42. https://doi.org/10.1039/C4TA04428B

Porzio, J., & Scown, C. D. (2021). Life-cycle assessment considerations for batteries and battery materials. *Advanced Energy Materials*, *11*(33), 2100771. https://doi.org/10.1002/aenm.202100771

Rey, I., Iturrondobeitia, M., Akizu-Gardoki, O., Minguez, R., & Lizundia, E. (2022). Environmental impact assessment of $Na_3V_2(PO_4)_3$ cathode production for sodium-ion batteries. *Advanced Energy and Sustainability Research*, *3*(8), 2200049. https://doi.org/10.1002/aesr.202200049

Rotolo, D., Hicks, D., & Martin, B. R. (2015). What is an emerging technology? *Research Policy*, *44*(10), 1827–1843. https://doi.org/10.1016/j.respol.2015.06.006

Rudnick, R. L., & Gao, S. (2014). 4.1 - Composition of the continental crust. In H. D. Holland & K. K. Turekian (Eds.), *Treatise on geochemistry* (pp. 1–51, 2nd ed.), Elsevier. https://doi.org/10.1016/B978-0-08-095975-7.00301-6

Sander-Titgemeyer, A., Risse, M., & Weber-Blaschke, G. (2023). Applying an iterative prospective LCA approach to emerging wood-based technologies: Three German case studies. *The International Journal of Life Cycle Assessment*, *28*, 495–515. https://doi.org/10.1007/s11367-023-02139-z

Schaubroeck, T., Schaubroeck, S., Heijungs, R., Zamagni, A., Brandão, M., & Benetto, E. (2021). Attributional & consequential life cycle assessment: Definitions, conceptual characteristics and modelling restrictions. *Sustainability*, *13*(13), 7386. https://doi.org/10.3390/su13137386

Schneider, S. F., Bauer, C., Novák, P., & Berg, E. J. (2019). A modeling framework to assess specific energy, costs and environmental impacts of Li-ion and Na-ion batteries. *Sustainable Energy & Fuels*, *3*(11), 3061–3070. https://doi.org/10.1039/C9SE00427K

Shiyou, L., Wenbo, L., Xiaoling, C., Chunlei, L., Yamin, H., Li, Y., Peng, W., Jie, W., & Youan, W. (2019). *Synthesis method and application of sodium bis(oxalato)borate* (Patent No CN110305153A). https://worldwide.espacenet.com/patent/search/family/068082611/publication/CN110305153A?q=pn%3DCN110305153A

Sonderegger, T., Berger, M., Alvarenga, R., Bach, V., Cimprich, A., Dewulf, J., Frischknecht, R., Guinée, J., Helbig, C., Huppertz, T., Jolliet, O., Motoshita, M., Northey, S., Rugani, B., Schrijvers, D., Schulze, R., Sonnemann, G., Valero, A., Weidema, B. P., & Young, S. B. (2020). Mineral resources in life cycle impact assessment—part I: A critical review of existing methods. *The International Journal of Life Cycle Assessment*, *25*(4), 784–797. https://doi.org/10.1007/s11367-020-01736-6

Sovacool, B. K. (2019). The precarious political economy of cobalt: Balancing prosperity, poverty, and brutality in artisanal and industrial mining in the Democratic Republic of the Congo. *The Extractive Industries and Society*, *6*(3), 915–939. https://doi.org/10.1016/j.exis.2019.05.018

Sun, X., Luo, X., Zhang, Z., Meng, F., & Yang, J. (2020). Life cycle assessment of lithium nickel cobalt manganese oxide (NCM) batteries for electric passenger vehicles. *Journal of Cleaner Production*, *273*, 123006. https://doi.org/10.1016/j.jclepro.2020.123006

Tapia-Ruiz, N., Armstrong, A. R., Alptekin, H., Amores, M. A., Au, H., Barker, J., Boston, R., Brant, W. R., Brittain, J. M., Chen, Y., Chhowalla, M., Choi, Y.-S., Costa, S. I. R., Ribadeneyra, M. C., Cussen, S. A., Cussen, E. J., David, W. I. F., Desai, A. V., Dickson, S. A. M., … Younesi, R. (2021). 2021 roadmap for sodium-ion batteries. *Journal of Physics: Energy*, *3*(3), 031503. https://doi.org/10.1088/2515-7655/ac01ef

Trotta, F., Wang, G. J., Guo, Z., Xu, Z., Ribadeneyra, M. C., Au, H., Edge, J. S., Titirici, M. M., & Lander, L. (2022). A comparative techno-economic and lifecycle analysis of biomass-derived anode materials for lithium- and sodium-ion batteries. *Advanced Sustainable Systems*, *6*(6), 2200047. https://doi.org/10.1002/adsu.202200047

Usiskin, R., Lu, Y., Popovic, J., Law, M., Balaya, P., Hu, Y.-S., & Maier, J. (2021). Fundamentals, status and promise of sodium-based batteries. *Nature Reviews Materials*, *6*(11), 1020–1035. https://doi.org/10.1038/s41578-021-00324-w

Vaalma, C., Buchholz, D., Weil, M., & Passerini, S. (2018). A cost and resource analysis of sodium-ion batteries. *Nature Reviews Materials*, *3*(4), 18013. https://doi.org/10.1038/natrevmats.2018.13

van der Hulst, M. K., Huijbregts, M. A. J., van Loon, N., Theelen, M., Kootstra, L., Bergesen, J. D., & Hauck, M. (2020). A systematic approach to assess the environmental impact of emerging technologies: A case study for the GHG footprint of CIGS solar photovoltaic laminate. *Journal of Industrial Ecology*, *24*(6), 1234–1249. https://doi.org/10.1111/jiec.13027

Vanholme, B., Desmet, T., Ronsse, F., Rabaey, K., Van Breusegem, F., De Mey, M., Soetaert, W., & Boerjan, W. (2013). Towards a carbon-negative sustainable bio-based economy. *Frontiers in Plant Science*, *4*, 174. https://doi.org/10.3389/fpls.2013.00174

van Oers, L., Guinée, J. B., & Heijungs, R. (2020). Abiotic resource depletion potentials (ADPs) for elements revisited—Updating ultimate reserve estimates and introducing time series for production data. *The International Journal of Life Cycle Assessment*, *25*(2), 294–308. https://doi.org/10.1007/s11367-019-01683-x

Vieira, M. D. M., Ponsioen, T. C., Goedkoop, M. J., & Huijbregts, M. A. J. (2017). Surplus ore potential as a scarcity indicator for resource extraction. *Journal of Industrial Ecology*, *21*(2), 381–390. https://doi.org/10.1111/jiec.12444

Wang, L., Li, H., Xin, S., He, P., Cao, Y., Li, F., & Hou, X. (2014). Highly efficient synthesis of diethyl carbonate via one-pot reaction from carbon dioxide, epoxides and ethanol over KI-based binary catalyst system. *Applied Catalysis A: General*, *471*, 19–27. https://doi.org/10.1016/j.apcata.2013.11.031

Wellings, J. (2021). *Supercapacitor electrodes, life cycle assessment of lithium-ion and sodium-ion battery packs: Innovation report*. University of Warwick. https://wrap.warwick.ac.uk/172888/

Wernet, G., Hellweg, S., & Hungerbühler, K. (2012). A tiered approach to estimate inventory data and impacts of chemical products and mixtures. *The International Journal of Life Cycle Assessment*, *17*(6), 720–728. https://doi.org/10.1007/s11367-012-0404-0

Wiedeman, O. F., Saunders, K. W., & O'connor, M. N. (1972). *Production of alkali metal ferrocyanide* (Patent No US3695833A). https://patents.google.com/patent/US3695833A/en

Xiaoming, P., Guocai, Q., & Guangping, S. (2013). *Preparation method of triethyl phosphate* (Patent No CN103374028A). https://patents.google.com/patent/CN103374028A/en

Xie, F., Xu, Z., Guo, Z., & Titirici, M.-M. (2020). Hard carbons for sodium-ion batteries and beyond. *Progress in Energy*, *2*(4), 042002. https://doi.org/10.1088/2516-1083/aba5f5

Xu, C., Dai, Q., Gaines, L., Hu, M., Tukker, A., & Steubing, B. (2020). Future material demand for automotive lithium-based batteries. *Communications Materials*, *1*(1), 99. https://doi.org/10.1038/s43246-020-00095-x

Yang, Y. (2019). A unified framework of life cycle assessment. *The International Journal of Life Cycle Assessment*, *24*(4), 620–626. https://doi.org/10.1007/s11367-019-01595-w

Zackrisson, M. (2021). *Life cycle assessment of electric vehicle batteries and new technologies*. KTH Royal Institute of Technology. https://kth.diva-portal.org/smash/record.jsf?pid=diva2%3A1554513&dswid=-1773

Zavalij, P. Y., Yang, S., & Whittingham, M. S. (2003). Structures of potassium, sodium and lithium bis(oxalato)borate salts from powder diffraction data. *Acta Crystallographica. Section B: Structural Crystallography and Crystal Chemistry*, *59*(Pt 6), 753–759. https://doi.org/10.1107/s0108768103022602

Zou, F., & Manthiram, A. (2020). A review of the design of advanced binders for high-performance batteries. *Advanced Energy Materials*, *10*(45), 2002508. https://doi.org/10.1002/aenm.202002508

SUPPORTING INFORMATION

Additional supporting information can be found online in the Supporting Information section at the end of this article.

How to cite this article: Wickerts, S., Arvidsson, R., Nordelöf, A., Svanström, M., & Johansson, P. (2023). Prospective life cycle assessment of sodium-ion batteries made from abundant elements. *Journal of Industrial Ecology*, 1–14. https://doi.org/10.1111/jiec.13452